Molecular Alignment and Rashba Splitting in Organometal Halide Perovskite $CH_3NH_3PbI_3$ Absorbers

Junwen Li[1,2] and Paul M. Haney[1]

[1.] Center for Nanoscale Science and Technology, National Institute of Standards and Technology, Gaithersburg, MD 20899, USA

[2.] Maryland Nano-Center, University of Maryland, College Park, MD 20742, USA

***Abstract* — Organometal halide perovskite $CH_3NH_3PbI_3$ solar cells have witnessed unprecedented progress in power conversion efficiency, reaching more than 20 % within 5 years. Despite this rapid progress, there remain open questions about the basic properties of these materials, such as the role of the polar molecule CH_3NH_3 (methylammonium), and the possible existence of ferroelectric ordering, and its role in device operation. Using first-principles density-functional theory, we investigated the effect of molecular alignment on the electronic structure. We find that the molecular alignment significantly modifies the near-gap states indirectly through the induced structural distortion of the $(PbI_6)^{4-}$ octahedron. The reduction in symmetry due to this distortion, combined with strong spin-orbit coupling of Pb, leads to a Rashba-like splitting of valence and conduction bands. This in turn leads to reduction of the degeneracy of the valence and conduction bands. These results imply that the electrical and optical properties are highly sensitive to ordering of the CH_3NH_3 dipole orientation.**

***Index Terms* — organometal halide perovskite, molecular alignment, Rashba splitting.**

I. Introduction

Organometal halide perovskites have recently attracted a great deal of attention because of their exceptional power conversion efficiency. The current record efficiency is more than 20 %, following an unprecedented pace of development since being first employed as photovoltaic absorbers in 2009 with an efficiency of 3.8 % [1]-[2]. The high efficiency is attributed to the optimal band gap (≈1.5 eV), high absorption coefficient, efficient charge transport properties, and long charge carrier diffusion length of over 100 nm for $CH_3NH_3PbI_3$ and 1 μm for mixed perovskite $CH_3NH_3PbI_{3-x}Cl_x$ [3]-[4]. In addition to the exceptional performance in power conversion efficiency, these perovskite materials exhibit many unusual characteristics, among which the anomalous hysteresis in $J-V$ curve is of great interest [5]. The hysteretic behavior leads to a large discrepancy in the cell efficiency between the forward and reverse bias scans. The source and significance of the hysteretic behavior are still unclear, with proposals such as trapping and de-trapping of carriers, ionic motion driven by the applied potential, and ferroelectric ordering of the material [5-7]. Ferroelectric domains have been experimentally observed directly using piezo force microscopy on solution-processed $CH_3NH_3PbI_3$ perovskite thin films [8]. It has been proposed that the presence of ferroelectric domains would facilitate separation of electrons and holes, providing "ferroelectric highways" for efficient charge collection [9].

In this work, we focus on the effect of ferroelectric ordering on the electronic structure. Ferroelectric order breaks inversion symmetry. It's well known that the presence of strong spin-orbit coupling, combined with breaking of inversion symmetry leads to a Rashba splitting of the electronic states [10]. This alters the electronic structure near the band gap, which can have significant impact on the optical and electronic material properties.

The ferroelectric polarization is derived from two distinct features of the lattice structure. One is the alignment of the methylammonia molecules' dipole moments. The other is associated with the structural distortion of the inorganic framework. The Rashba splitting is a result of these two contributions. In this paper, we investigated the effect of molecular alignment on the electronic structure and found that the molecular alignment leads to large Rashba splitting through the alignment-induced structural distortion in the $(PbI_6)^{4-}$ octahedron. Since the different molecular alignments have comparable energies, temperature may be used to tune the percentage of the ordering. We therefore, propose that the electronic structure and optical properties will change with varying temperatures if ferroelectric effects are present.

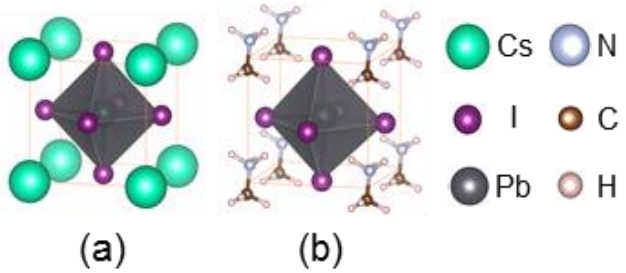

Fig. 1. Schematic of cubic perovskite (a) $CsPbI_3$ and (b) $CH_3NH_3PbI_3$. The polar $CH_3NH_3^+$ ions are aligned along <001> direction.

II. Atomic Structures

Experimentally, the perovskite crystals exhibit three different structural phases, namely cubic ($Pm\bar{3}m$), tetragonal ($I4/mcm$), and orthorhombic ($Pnma$) depending on the temperature [11]. To focus on the effect of molecular alignment, we choose the cubic phase and align the molecules along <001> direction which is of the lowest energy among several possible alignments [12]. The lattice constant and atomic positions within the cubic unit cell were optimized using local density approximation in the form of norm-conserving pseudopotentials as implemented in Quantum-ESPRESSO [13] with an energy cutoff 80 Ry for the plane wave basis expansion and a $6 \times 6 \times 6$ grid for the Brillouin zone sampling. During relaxation, all atoms in the unit cell were allowed to move until the force on each atom is less than 0.5 eV/nm. The lattice constant is calculated to be a = 0.621 nm, in good agreement with the experimental result (a = 0.626 nm [14]) and also consistent with the structural determination with local density approximation which usually underestimates the lattice constant. Distortions of the $(PbI_6)^{4-}$ octahedron are observed and the Pb atom shifts away from the body center by 0.019 nm. For comparison, we also studied the $CsPbI_3$ with undistorted octahedron. The lattice constant is determined to be 0.619 nm, comparable to the experimental value of 0.629 nm [15].

III. Electronic Structures

We first consider the cubic $CsPbI_3$ with undistorted octahedron as a reference system and show in Fig. 2 the total and projected density of states without spin-orbit coupling included. Near the Fermi level, the conduction band states are derived from the *p* orbital of Pb while the valence band states are composed of the Pb *s* orbital and I *p* orbital. The electronic energy states derived from the Cs atom are mostly located more than 2 eV away from the Fermi level both within the valence and the conduction bands. $CH_3NH_3PbI_3$ has similar orbital contributions near the Fermi level. So the electronic and optical properties in the visible range are dominated by the orbitals of Pb and I atoms. Fig. 3(a) depicts the electronic structure of $CsPbI_3$ without spin-orbit coupling considered. Both the valence band maximum (VBM) and the conduction band minimum (CBM) are located at the *R* point [zone boundary, $(\pi/a, \pi/a, \pi/a)$]. The band structure of $CH_3NH_3PbI_3$ is similar to that of $CsPbI_3$, but with significant changes in the conduction band edges as shown in Fig. 3(b). The presence of aligned dipolar methylammonium and the octahedral distortion lift the degeneracy between p_x, p_y, and p_z orbitals. The gap becomes slightly indirect, with nearly degenerate energy states for CBM at *R* point.

Because of the heavy Pb atom, relativistic effects are expected to play an important role. We calculate the electronic structures of $CsPbI_3$ and $CH_3NH_3PbI_3$ with spin-orbit coupling included as shown in Fig. 3(c) and (d), respectively. In $CsPbI_3$ adding spin-orbit coupling splits degenerate conduction band states ($L = 1$) into lower $J = 1/2$ and upper $J = 3/2$ bands, whereas spin-orbit coupling has little effect on the valence band derived from the *s* orbital, leading to a $J = 1/2$ CBM and $S = 1/2$ VBM. The spin-orbit coupling also significantly reduces the band gap by 0.98 eV.

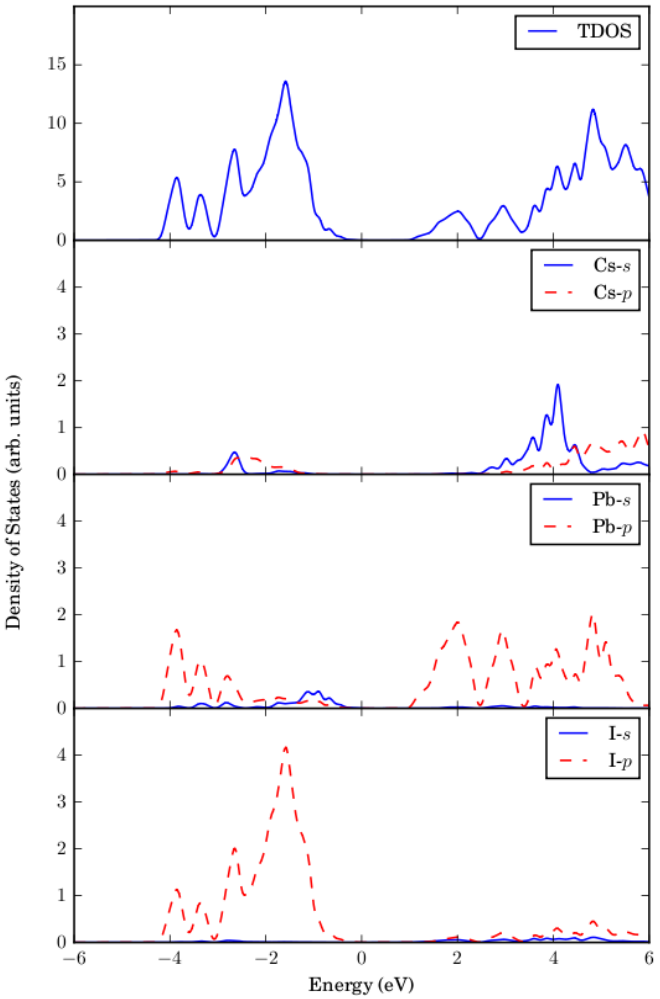

Fig. 2. Total and partial density of states projected onto *s* and *p* orbitals for $CsPbI_3$. The Fermi level is set to zero.

The effect of spin-orbit coupling in $CH_3NH_3PbI_3$ is more significant because of the ferroelectric polarization derived from the dipolar molecules alignment and ensuing structural distortion. Using the Berry phase approach, we find a polarization of 47.2 μC/cm^2. As discussed in the introduction, the interplay between spin-orbit coupling and inversion symmetry breaking results in Rashba splitting. As shown in Fig. 3(d), the electronic structure exhibits larger Rashba splitting for the conduction band and in Fig. 4 we show the Rashba-type spin distribution on the energy contours of 170 meV above the conduction band minimum in k_x-k_y plane. The asymmetry in conduction band and valence band may have impact on the absorbance, and radiative

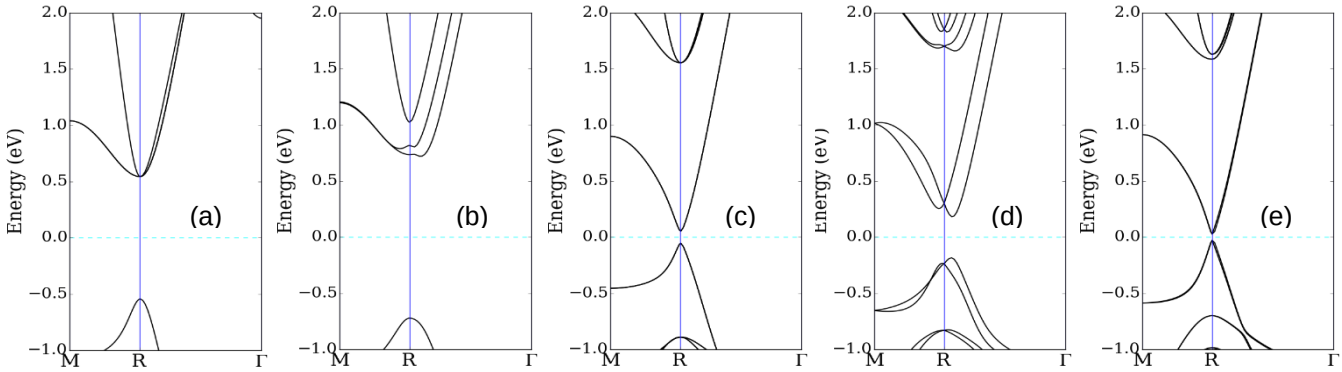

Fig. 3. Electronic structures of relaxed (a) cubic $CsPbI_3$ and (b) $CH_3NH_3PbI_3$ with ordered methylammonium ions and octahedral distortion, and without the consideration of spin-orbit coupling. (c) and (d) are the corresponding electronic structures with spin-orbit coupling included. (e) corresponds to the cubic $CH_3NH_3PbI_3$ with ordered methylammonium ions and no octahedral distortion.

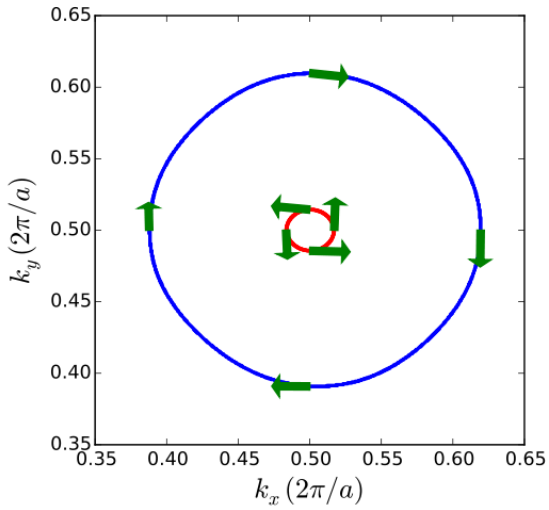

Fig. 4. In-plane spin distribution on the energy contours of 170 meV above the conduction band minimum. Arrows indicate the in-plane orientation and the length is proportional to the modulus of the spin.

recombination of photo-excited electron and hole charge carriers.

In order to gain insight on the relative importance of dipolar ordering versus the distortion of the $(PbI_6)^{4-}$ octahedron, we carried out simulations with a hypothetical model system in which we fixed the Pb in the body center and I atoms at face centers and aligned methylammonium along <001> direction. The polarization is calculated to be 51 μC/cm^2. Fig. 3(e) shows that the Rashba effect is nearly vanishing, suggesting that the octahedral distortion is the main cause of Rashba splitting. To understand this, we note that the Rashba splitting magnitude depends on the spin-orbit coupling strength and the degree of inversion symmetry breaking. In this material, the splitting is therefore determined by the asymmetry of the environment surrounding the Pb atom. In a symmetric octahedron with aligned dipoles, the screening of I ions leads to small change in the electrostatic potential around Pb atom and therefore reduced Rashba splitting. On the other hand, a distortion of the octahedron leads to a highly asymmetric environment for the Pb atom. For this reason, we conclude the alignment of the molecules is important for the band structure mostly due to the resulting distortion of the octahedron.

IV. Summary

In summary, we report on first-principles density-functional simulations on the effect of molecular alignment on the energy states near the Fermi level. We found that only the alignment of methylammonium ion dipoles alone does not significantly modify the near-gap states. However, accounting for the full relaxation of the atomic positions leads to an off-center displacement of the Pb atom which induces a much larger Rashba splitting. Therefore, the role of the methylammonium ions ordering on the electronic structure is indirect, and takes place through a structural change. Our finding suggests that engineering the octahedron directly or indirectly through tuning the molecules may be an effective route in tailoring the Rashba splitting and band gap nature. Additionally, these results suggest a strong dependence of optical properties, such as absorption, on the alignment of the methylammonium ions, and more generally on the symmetry of the octahedron. An observed dependence of the optical properties on temperature would be consistent with ferroelectric ordering, and would suggest that this effect plays an important role in the photovoltaic properties of this material.

ACKNOWLEDGEMENT

J. L. acknowledges support under the Cooperative Research Agreement between the University of Maryland and the National Institute of Standards and Technology Center for Nanoscale Science and Technology, Award 70NANB10H193, through the University of Maryland.

References

[1] A. Kojima, K. Teshima, Y. Shirai, and T. Miyasaka, "Organometal halide perovskites as visible-light sensitizers for photovoltaic cells," *J. Am. Chem. Soc.*, vol. 131, no. 17, pp. 6050–1, May 2009.

[2] Best Research Cell Efficiency Chart. http://www.nrel.gov/ncpv/images/efficiency_chart.jpg.

[3] S. D. Stranks, G. E. Eperon, G. Grancini, C. Menelaou, M. J. P. Alcocer, T. Leijtens, L. M. Herz, A. Petrozza, and H. J. Snaith, "Electron-hole diffusion lengths exceeding 1 micrometer in an organometal trihalide perovskite absorber," *Science*, vol. 342, no. 6156, pp. 341–4, Oct. 2013.

[4] G. Xing, N. Mathews, S. Sun, S. S. Lim, Y. M. Lam, M. Grätzel, S. Mhaisalkar, and T. C. Sum, "Long-range balanced electron- and hole-transport lengths in organic-inorganic $CH_3NH_3PbI_3$," *Science*, vol. 342, no. 6156, pp. 344–7, Oct. 2013.

[5] H. J. Snaith, A. Abate, J. M. Ball, G. E. Eperon, T. Leijtens, N. K. Noel, S. D. Stranks, J. T.-W. Wang, K. Wojciechowski, and W. Zhang, "Anomalous hysteresis in perovskite solar cells," *J. Phys. Chem. Lett.*, vol. 5, no. 9, pp. 1511–1515, May 2014.

[6] Z. Xiao, Y. Yuan, Y. Shao, Q. Wang, Q. Dong, C. Bi, P. Sharma, A. Gruverman, and J. Huang, "Giant switchable photovoltaic effect in organometal trihalide perovskite devices," *Nat. Mater.*, vol. 14, no. 2, pp. 193–198, Dec. 2014.

[7] C. C. Stoumpos, C. D. Malliakas, and M. G. Kanatzidis, "Semiconducting tin and lead iodide perovskites with organic cations: phase transitions, high mobilities, and near-infrared photoluminescent properties," *Inorg. Chem.*, vol. 52, no. 15, pp. 9019–38, Aug. 2013.

[8] Y. Kutes, L. Ye, Y. Zhou, S. Pang, B. D. Huey, and N. P. Padture, "Direct observation of ferroelectric domains in solution-processed $CH_3NH_3PbI_3$ perovskite thin films," *J. Phys. Chem. Lett.*, vol. 5, no. 19, pp. 3335–3339, Oct. 2014.

[9] J. M. Frost, K. T. Butler, F. Brivio, C. H. Hendon, M. van Schilfgaarde, and A. Walsh, "Atomistic origins of high-performance in hybrid halide perovskite solar cells," *Nano Lett.*, vol. 14, no. 5, pp. 2584–90, May 2014.

[10] L. Petersen and P. Hedegård, "A simple tight-binding model of spin–orbit splitting of *sp*-derived surface states," *Surf. Sci.*, vol. 459, no. 1–2, pp. 49–56, Jul. 2000.

[11] Y. Kawamura, H. Mashiyama, and K. Hasebe, "Structural study on cubic–tetragonal transition of $CH_3NH_3PbI_3$," *J. Phys. Soc. Japan*, vol. 71, no. 7, pp. 1694–1697, Jul. 2002.

[12] J. M. Frost, K. T. Butler, and A. Walsh, "Molecular ferroelectric contributions to anomalous hysteresis in hybrid perovskite solar cells," *APL Mater.*, vol. 2, no. 8, p. 081506, Aug. 2014.

[13] P. Giannozzi, S. Baroni, N. Bonini, M. Calandra, R. Car, C. Cavazzoni, D. Ceresoli, G. L. Chiarotti, M. Cococcioni, I. Dabo, A. Dal Corso, S. de Gironcoli, S. Fabris, G. Fratesi, R. Gebauer, U. Gerstmann, C. Gougoussis, A. Kokalj, M. Lazzeri, L. Martin-Samos, N. Marzari, F. Mauri, R. Mazzarello, S. Paolini, A. Pasquarello, L. Paulatto, C. Sbraccia, S. Scandolo, G. Sclauzero, A. P. Seitsonen, A. Smogunov, P. Umari, and R. M. Wentzcovitch, "QUANTUM ESPRESSO: a modular and open-source software project for quantum simulations of materials," *J. Phys. Condens. Matter*, vol. 21, no. 39, p. 395502, Sep. 2009.

[14] T. Baikie, Y. Fang, J. M. Kadro, M. Schreyer, F. Wei, S. G. Mhaisalkar, M. Graetzel, and T. J. White, "Synthesis and crystal chemistry of the hybrid perovskite $(CH_3NH_3)PbI_3$ for solid-state sensitised solar cell applications," *J. Mater. Chem. A*, vol. 1, no. 18, p. 5628, Apr. 2013.

[15] D. M. Trots and S. V. Myagkota, "High-temperature structural evolution of caesium and rubidium triiodoplumbates," *J. Phys. Chem. Solids*, vol. 69, no. 10, pp. 2520–2526, Oct. 2008.